Journal of Geophysical Research: Biogeosciences

RESEARCH ARTICLE

10.1029/2018JG004385

Key Points:
- Coralline algal Mg/Ca ratios have a strong correlation with regional SST
- Coralline algae enable reconstruction of a 42-year temperature time series

Supporting Information:
- Figure S1
- Data Set S1

Correspondence to:
S. Williams,
siobhan.williams@mail.utoronto.ca

Citation:
Williams, S., Halfar, J., Zack, T., Hetzinger, S., Blicher, M., Juul-Pedersen, T., et al. (2018). Coralline algae archive fjord surface water temperatures in Southwest Greenland. *Journal of Geophysical Research: Biogeosciences*, *123*, 2617–2626. https://doi.org/10.1029/2018JG004385

Received 6 JAN 2018
Accepted 18 JUL 2018
Accepted article online 28 JUL 2018
Published online 30 AUG 2018

Coralline Algae Archive Fjord Surface Water Temperatures in Southwest Greenland

Siobhan Williams[1], Jochen Halfar[1], Thomas Zack[2], Steffen Hetzinger[3], Martin Blicher[4], Thomas Juul-Pedersen[4], Andreas Kronz[5], Brice Noël[6], Michiel van den Broeke[6], and Willem Jan van de Berg[6]

[1]CPS-Department, University of Toronto Mississauga, Mississauga, Ontario, Canada, [2]Department of Earth Sciences, University of Gothenburg, Gothenburg, Sweden, [3]Institut für Geologie, Universität Hamburg, Hamburg, Germany, [4]Greenland Climate Research Centre, Greenland Institute of Natural Resources, Nuuk, Greenland, [5]Geowissenschaftliches Zentrum, Universität Göttingen, Göttingen, Germany, [6]Institute for Marine and Atmospheric Research Utrecht, Utrecht University, Utrecht, The Netherlands

Abstract One of the most dramatic signs of ongoing global change is the mass loss of the Greenland Ice Sheet and the resulting rise in sea level, whereby most of the recent ice sheet mass loss can be attributed to an increase in meltwater runoff. The retreat and thinning of Greenland glaciers has been caused by rising air and ocean temperatures over the past decades. Despite the global scale impact of the changing ice sheet balance, estimates of glacial runoff in Greenland rarely extend past several decades, thus limiting our understanding of long-term glacial response to temperature. Here we present a 42-year long annually resolved red coralline algal Mg/Ca proxy temperature record from a southwestern Greenland fjord, with temperature ranging from 1.5 to 4 °C (standard error = 1.06 °C). This temperature time series in turn tracks the general trend of glacial runoff from four West Greenland glaciers discharging freshwater into the fjord (all $p < 0.001$). The algal time series further exhibits significant correlations to Irminger Sea temperature patterns, which are transmitted to western Greenland fjords via the West Greenland Current. The 42-year long record demonstrates the potential of annual increment forming coralline algae, which are known to live up to 650 years and which are abundant along the Greenland coastline, for reconstructing time series of sea surface temperature.

1. Introduction

Since the mid-1990s, the relative importance of runoff as a cause of ice sheet mass loss has increased and, between 2009 and 2012, accounted for 84% of the increase in the rate of mass loss (Enderlin et al., 2014). Various authors have suggested that retreat in tidewater glaciers is largely driven by increases in sea surface temperature (SST; Drinkwater et al., 2014; Howat et al., 2008; Kerr, 2000). A recently published map of Greenland's bedrock has found that 30–100% more glaciers than previously identified may be exposed to Atlantic water (Morlighem et al., 2017). These glaciers might therefore experience an increase in calving, ice front retreat, and glacier thinning with rising SST (Enderlin et al., 2013; Howat et al., 2008). Under higher SST conditions, as a result of global warming (Hanna et al., 2008), there is typically more runoff from the surface of glaciers since air and water temperatures are coupled (Moore & Demuth, 2001). SST in southwestern Greenland fjords is in part controlled by changes in the West Greenland Current and the presence of shallow subsurface Irminger Sea water masses (Buch et al., 2004; Figure 1).

While the regional oceanography is well understood, long-term instrumental observations are sparse in Greenland. Before the beginning of satellite observations in the 1980s, SSTs reconstructed with few in situ observations are available from the late 1800s (Rayner et al., 2003), while modeled glacial runoff estimates extend to the late 1950s (Regional Atmospheric Climate Model, RACMO 2.3p2; ECMWF-IFS, 2008; Noël et al., 2018). Hence, the length of both temperature data sets and glacial runoff information is too short to assess century-scale variability.

The main objective of this study is to reconstruct fjord water temperatures, which in turn are influenced by the interaction with the West Greenland Current (Mortensen et al., 2013, 2014). This current derives its water-mass properties from a mixture of Irminger Sea and East Greenland Current water. To obtain our objective, we have investigated the potential of a proxy-based reconstruction of surface water conditions in a West

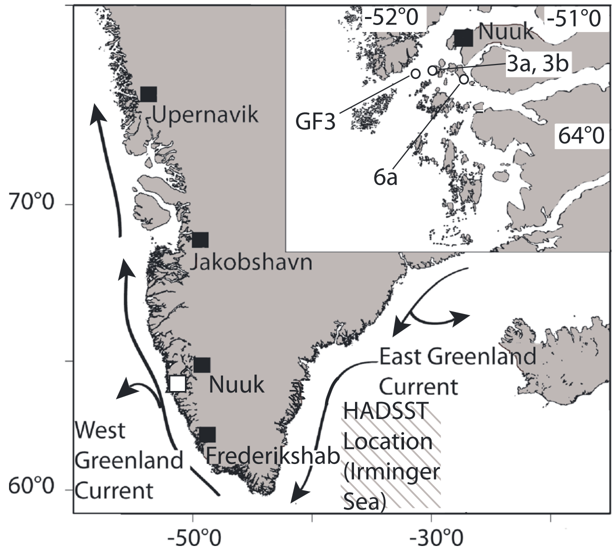

Figure 1. Location of sample collection and monitoring sites in Godthåbsfjord, Southwest Greenland (marked by a white square) as well as four major marine terminating glaciers (marked by black squares). Inset of Godthåbsfjord depicts oceanographic monitoring station (GF3) and locations of samples 6a, 5c, 3a, and 3b. Also shown is the location of the Irminger Sea HADISST1 temperature reconstruction grid box used in this study.

Greenland fjord. While our record only covers 42 years, the coralline algal species *Clathromorphum compactum* (Kjellman) Foslie (1898), which was used for this study, can have a lifespan of up to 650 years (Halfar et al., 2013). *Clathromorphum compactum*'s annual increment forming (Figure 2) skeleton is constructed with high-magnesium calcite crystals and has previously been calibrated and used as a multicentury paleotemperature proxy recorder in the North Atlantic (Halfar et al., 2013; Hetzinger et al., 2018). *Clathromorphum* sp. grows on rocky substrate, has a wide distribution throughout the arctic and subarctic coasts (Adey et al., 2013), and has been described from numerous locations along the west Greenland coast from the southern tip as far north as Upernavik (Figure 1; Jørgensbye & Halfar, 2016).

2. Materials and Methods

2.1. Sample Collection and Site Description

Clathromorphum compactum samples were live collected from the outer portion of Godthåbsfjord (Figure 1), in summer 2013 by divers at approximately 10-m depth. Two shorter-lived specimens (16- and 34-year lifespans: samples 3a and 3b, respectively) were collected 3 km from oceanographic monitoring station GF3 (64°12′N, 51°88′W) in order to establish a local species-specific Mg/Ca proxy-temperature calibration (Figure 1). At GF3, which was maintained by MarineBasis-Nuuk as part of the Greenland Ecosystem Monitoring program, temperature, salinity, and isotopic seawater composition were recorded monthly since 2005. Longer-lived specimens (samples 5c and 6a) with lifespans of >40 years were collected 10 km east of the oceanographic monitoring station.

Summer conditions in Godthåbsfjord (Figure 1) are characterized by a relatively fresh surface layer in comparison to subsurface waters, as a result of glacier-derived freshwater runoff from land and precipitation (Mortensen et al., 2011). Temperature and salinity vary within the fjord with distance from the sources of freshwater. In the winter, surface-water salinities increase (from 5–28 in summer to 31–33 in winter, measured at a mooring in the fjord [64°40′N, 50°56′W] approximately 60 km from the Akugdlerssûp Sermia glacier), and temperatures at the mooring decrease from 10 °C in summer to below 0 °C in winter (Mortensen et al., 2011). The fresh surface layer is thinner in the summer (~5 m) than the winter (~30 m) because in summer, it is formed by runoff, while winter surface water is a combination of runoff and surface cooling (Mortensen

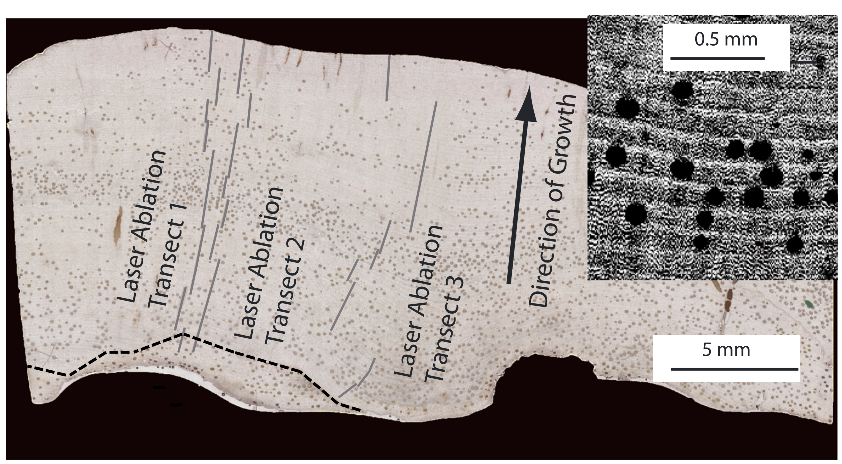

Figure 2. Cross section of *Clathromorphum compactum* (sample 6a) showing position of laser ablation inductively coupled plasma mass spectrometry transects. Dotted line at bottom of sample indicates growth hiatus, and data analyzed below the hiatus were not included in Mg/Ca record. Inset shows detail of annual growth increments and conceptacle cavities (dark circles).

et al., 2011). Over the course of the year, there are relatively large influxes of freshwater into the fjord derived from tidewater glaciers Kangiata Nunaata Sermia, Akugdlerssûp Sermia glacier, and Narsap Sermia, but 2.5 times more freshwater is introduced from May to November than in the winter (Mortensen et al., 2013). Typically, in midsummer, water is transported in the subsurface layer at peak velocities into the fjord, toward the glaciers Kangiata Nunaata Sermia, Akugdlerssûp Sermia, and Narsap Sermia. By late summer, this transport becomes slower and deeper, while outside of the summer months, velocities are further reduced, and the inflow of coastal water and outflow of water inside the fjord are deep (Mortensen et al., 2014).

2.2. Analysis

Samples were sectioned perpendicular to the direction of growth and polished using diamond suspension to a grit size of 1 μm. The software geo. TS (Olympus Soft Imaging Systems) was utilized with an automated sampling stage on a reflected light microscope to produce two-dimensional maps of the polished thick sections. These high-resolution composite images were used to establish an age model based on annual growth increments and to select linear transects across growth increments for geochemical analysis (for details, see Hetzinger et al., 2009).

Mg/Ca composition along the predefined transects was measured with laser ablation inductively coupled plasma mass spectrometry (LA-ICP-MS) using a New Wave NWR 213 laser ablation system coupled with an Agilent 8800 Quadrupole ICP-MS in the Earth Sciences department at Gothenburg University. On sample 6a, three parallel LA-ICP-MS line transects were measured. On samples 3a, 3b, and 5c, two transects were analyzed extending from the top to the oldest visibly unaltered material (Figure 2). Each sample underwent a preablation step to remove surface contaminants, and the transects were divided into segments to avoid conceptacles (uncalcified reproductive structures; Figure 2), which yield Mg/Ca signals that do not represent temperatures. Each segment of the Mg/Ca transects overlaps with the next segment by 1–2 years, and the Mg/Ca data obtained from overlapping transects were averaged. For measurements of ^{24}Mg and ^{43}Ca (for quantification of Mg and Ca, respectively), the laser energy was approximately 6 J/cm^2, laser frequency was 10 Hz, and carrier gas was helium (5 ml/min nitrogen mixed in between the laser chamber and the ICP-MS). The laser spot was 50 × 50 μm, and the sample stage advanced at a speed of 10 μm/s. The internal standard was ^{43}Ca, using calcium concentrations measured by solution inductively coupled plasma optical emission spectrometry (Hetzinger et al., 2009). NIST SRM 610 glass (U.S. National Institute of Standard and Technology Standard Reference Material) was analyzed as an external standard. Hourly measurements of NIST SRM 610 were taken to quantify instrumental drift over the course of the single day of analyses. GLITTER 4.4.4 (Macquarie University, Sydney) was used for data reduction. Relative standard deviation for analysis of NIST SRM 610 glass is Mg/Ca = 0.99%. Detection limits were Mg = 0.07 ppm and Ca = 94.25 ppm.

2.3. Data Reduction

The seasonal cyclicity of Mg/Ca ratios was used to generate age models by marking the annual minimum Mg/Ca as February and the maximum as August of every year in the time series, since SST from HADISST1 (see section 2.4) demonstrates that these months represent the mean lowest and highest temperatures annually in a region outside of Godthåbsfjord (Lon = −56 to −51°W; Lat = 60 to 65°N). Once seasonal markers were identified for each year, the program AnalySeries 2.0.8 (Paillard et al., 1996) was used to resample the time series to 12 equidistant Mg/Ca data points/year resolution. These points were assigned to months of the year despite the fact that algal growth rates are likely faster in summer than winter. However, to date, intra-annual growth rates in *C. compactum* are poorly constrained. Using the 12 points/year resolution data, multiple (2–3) transects from each sample were averaged to form a single chronology. Averaging multiple transects and samples improves the climate signal of coralline algae because the averaging diminishes noise in the record caused by conditions other than temperature, such as local and temporal shading or grazing (Hetzinger et al., 2018; B. Williams et al., 2014). The two shorter-lived samples (3a and 3b) collected within 3 km GF3 (the oceanographic monitoring station) were used for calibration (a total of four LA-ICP-MS transects). The Mg/Ca data from these samples were averaged to produce a single record and then binned by Mg/Ca ratio levels in 0.002 increments (from 0.089 to 0.150). A linear regression between this Mg/Ca record and the in situ water temperatures from 12-m depth was carried out to generate a site-specific Mg/Ca proxy-temperature calibration equation. The need for site specific *Clathromorphum* sp. Mg/Ca-temperature calibrations has previously been established by B. Williams et al. (2014). Finally, the calibration was applied to calculate temperature from Mg/Ca data obtained from the two longer-lived samples (5c and 6a), which were collected 10 km from the

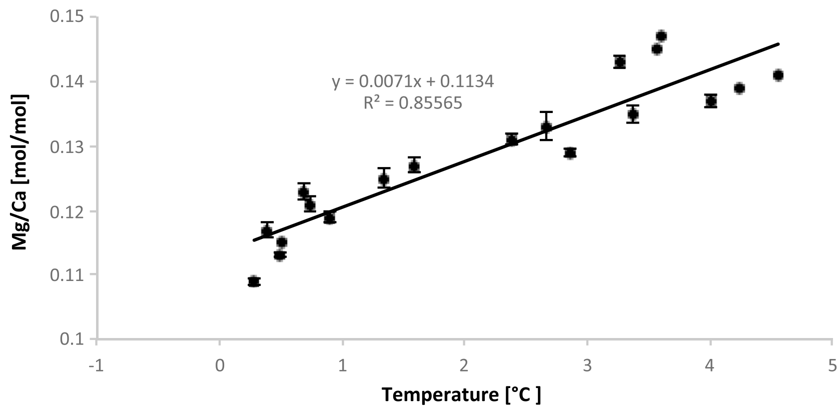

Figure 3. Linear regression between monthly algal Mg/Ca (± 2σ) of calibration samples and in situ water temperature measurements (station GF3) over 6 years (binned by aggregating the Mg/Ca values in groups of 0.002 increments from 0.089 to 0.150).

oceanographic station. An averaged record from the two longer-lived samples, consisting of a total of five transects, was used for comparisons with SST. The two longer-lived samples provided similar reconstruction patterns (correlation coefficient of 5-year running averages between samples 5c and 6a: $r = 0.68$, $n = 38$, $p = 0.001$).

2.4. Instrumental and Model Data

Temperature and salinity observations from 2005 to 2012 were obtained from the Greenland Institute of Natural Resources collected at GF3 in Godthåbsfjord at 12-m depth (Figure 1). For a longer term record from this area, Reynolds SST reanalysis data (1982–2012) for a 1° × 1° square (Lon = −52 to −51°W; Lat = 62 to 63°N) were used (Reynolds et al., 2002). The coralline Mg/Ca record was also compared to modeled glacial melt runoff (for model details, see Noël et al., 2015) estimated from four regions with major Southwest Greenland outlet glaciers: Frederikshab (Lon = −49.7 to −49.1°W; Lat = 62.6 to 62.9°N), Nuuk, including glaciers Kangiata Nunaata Sermia, Akugdlerssûp Sermia, and Narsap Sermia (Lon = −50.0 to −49.4°W; Lat = 63.2 to 63.7°N), Jakobshavn (Lon = −49.5 to −48.9°W; Lat = 69.1 to 69.4°N), and Upernavik (Lon = −54.6 to −54.0°W; Lat = 72.8 to 73.1°N; Figure 1). HADISST1 SST data for a 5° × 5° square outside of Godthåbsfjord (Lon = −56 to −51°W; Lat = 60 to 65°N) and upstream in the Irminger Sea (Lon = −32 to −27°W; Lat = 58 to 63°N) were used for temperature correlations (1970–2012; Rayner et al., 2003; Figure 1). Correlations were calculated between coralline algal data, RACMO 2.3p2, and HADISST1 data. Air temperatures were obtained from the locations of Akugdlerssûp Sermia from CRUTEM4, a data set derived from air temperatures near the land surface and recorded by weather stations, developed, and maintained by the Met Office's (UK) Climatic Research Unit (Jones & Moberg, 2003). Nuuk air temperatures (annual) from 1970 to 2012 were retrieved from the Global Historical Climatology Network (Peterson & Vose, 1997). Low frequency trends of SST and glacier data were calculated using singular spectrum analysis in the program kSpectra (Vautard et al., 1992).

3. Results

3.1. Temperature Reconstruction

Algal samples collected near the Greenland Institute of Natural Resources oceanographic station GF3 show a statistically significant relationship between binned monthly resolved Mg/Ca ratios and instrumental temperatures from 2005 to 2012 ($r = 0.91$, $p < 0.001$; Figure 3). The Mg/Ca ratio outliers shown in Figure 3 are likely the result of a combination of biological variability and other environmental influences, such as light, on *Clathromorphum* Mg/Ca ratios (Moberly, 1968). Since specimen variability of Mg/Ca is common in *Clathromorphum*, it has been determined that averaging of multiple specimens reduces the impact of outliers on the time series (Hetzinger et al., 2018; B. Williams et al., 2014; S. Williams et al., 2018). This was taken into account in our longer time series by averaging five transects from two samples. The following equation defines the relationship between temperature and Mg/Ca for *C. compactum* from Godthåbsfjord (based on

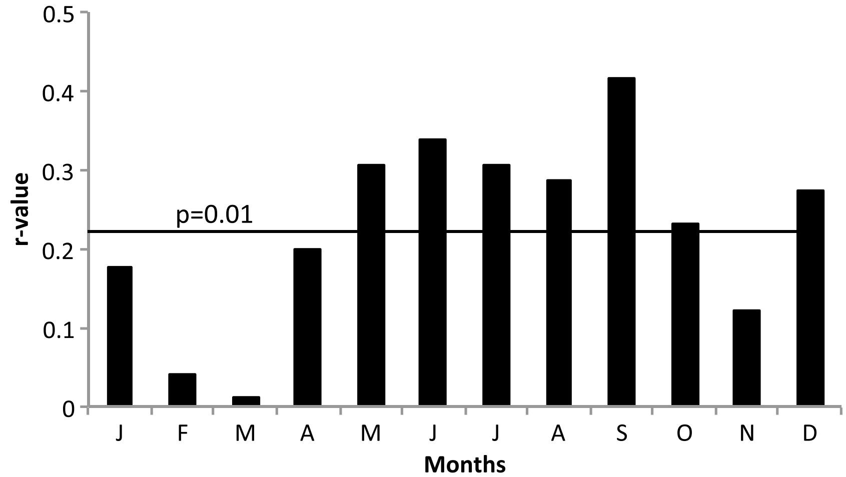

Figure 4. Correlations between annual coralline algal Mg/Ca and monthly Godthåbsfjord sea surface temperature. Correlation coefficients calculated using annual Mg/Ca ratios and monthly Reynolds sea surface temperature values for all 42 years of algal record (samples 5c and 6a averaged).

monthly data): Mg/Ca = 0.0068 T [°C] + 0.11. This calibration yields a 1.06 °C standard error in temperature and defines the resolution of the calibration.

A comparison of annual algal Mg/Ca of the two longer-lived samples with Godthåbsfjord Reynolds SST reveals that *C. compactum* Mg/Ca ratios have significant relationships with May–October SST, with the strongest relationships in September, which is a similar pattern to the one found in Maine, United States, and Newfoundland *C. compactum* (Figure 4; Gamboa et al., 2010; Halfar et al., 2008). This stronger correlation from May to October is a result of the algae exhibiting higher growth rates with the increase in both temperatures and insolation in summer. During the dark cold winter months, growth of high latitude *Clathromorphum compactum* algae is significantly reduced or halted (Halfar et al., 2013). Since the correlations are the strongest between the Mg/Ca chronology and May–October Reynolds SST data, these months were chosen for temperature comparisons with the 42-year algal temperature record. This record was generated by averaging Mg/Ca ratios from five transects from two longer-lived samples and converting those to temperature using the above equation. Nuuk peak growing season air temperature variations (May–October) are related with the coralline algal record (r = 0.46, n = 42, p = 0.001; Figure 5). This correlation was found to be statistically significant at the 99% confidence level after taking into account the temporal autocorrelation of the underlying time series (p_{adj} = 0.01, adjusted for the loss of degrees of freedom, all subsequent p_{adj} are adjusted for autocorrelation). A p value of <0.01 are commonly used in algalchronological studies to determine months of significant correlations (e.g., Gamboa et al., 2010; Halfar et al., 2008). Nuuk summer air temperatures (Figure 5) are on average 3 °C warmer than the coralline algal summer temperatures derived from approximately 10-m depth, and the air temperatures exhibit more variability than the coralline algal record. The greater variability in air temperatures may be caused by either the ocean buffering temperature resulting in higher atmospheric temperature variability than oceanic variability or less variability in the algal record may be a result of the ±1.06 °C standard error of our calibration.

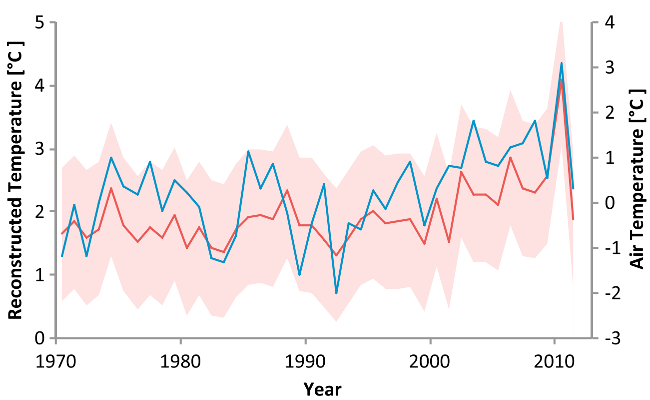

Figure 5. Annually resolved Nuuk May–October air temperatures (blue line) compared to algal Mg/Ca-derived reconstructed water temperatures (red line). Shaded area shows error of coralline algal reconstruction (standard error of calibration).

Algal Mg/Ca ratios are significantly related to SST (r = 0.64, $p < 0.001$, $p_{adj} < 0.001$, 1970–2012; Figure 7) outside of Godthåbsfjord (HADISST1, Lon = −56 to −51°W; Lat = 60 to 65°N). A spatial correlation analysis between algal Mg/Ca and North Atlantic SST (1970–2012, May–September HADISST1) reveals significant relationships of the south and west of Iceland in the Irminger Sea (Figure 6). This spatial correlation extends into the region of the West Greenland Current and weakens at the southern tip of Greenland and as the current travels north along the

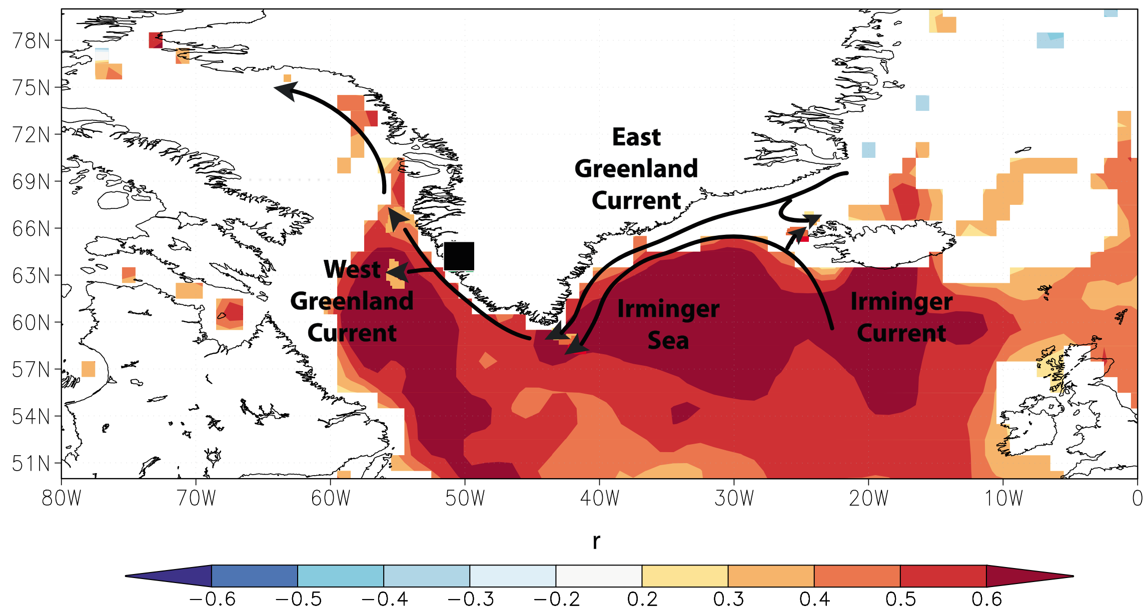

Figure 6. Spatial correlations between HADISST1 and algal Mg/Ca (1970–2012). Colors indicate correlation coefficient. Black square marks Godthåbsfjord collection site.

west coast of Greenland past Godthåbsfjord, and in the Labrador Sea. Irminger Sea HADISST1 (January–June) and peak growing season coralline algal temperatures (May–October) are significantly correlated throughout the entire time series with a 4-month lag allowing for the water to travel between the Irminger Sea and Godthåbsfjord (r = 0.42, $p < 0.001$, $p_{\mathrm{adj}} < 0.001$; Cuny et al., 2002). While the patterns of decadal-scale temperature variability of both records are similar, Irminger Sea SST is on average 5.5 °C warmer than the coralline algal temperatures calculated from Godthåbsfjord.

3.2. Glacial Runoff

Glacial runoff of some of the largest glaciers in southwest Greenland, Upernavik, Jakobshavn, Nuuk, and Frederikshab (Figure 1; Xu et al., 2012) correlates with both the regional SST and local air temperatures (all p values < 0.001). Coralline Mg/Ca is related to water and air temperature and thus also indirectly linked to runoff (all p values < 0.001). Low frequency trends of glacial runoff from the four tidewater glaciers are similar to those of the coralline algae (Figure 7c). At all four locations, the glacial runoff estimates remain relatively constant until the steep increase between 1995 and 2012 corresponding to the algal Mg/Ca increase in the 1990s (Figure 7c). Despite the algal and glacial runoff records showing the same overall trend, the annual patterns do not always match and occasionally show inverse trends.

4. Discussion

4.1. Temperature Reconstruction

The correlation between coralline algal reconstructed temperature variability and the Irminger Sea SST illustrates the link between polar water originating in the Arctic Ocean and water conditions at the mouth of Godthåbsfjord. As the Arctic Ocean-derived water travels south along the east coast of Greenland to the Irminger Sea (Figure 1), it is modified by local water masses (Mortensen et al., 2011). From the Irminger Sea, the water continues to travel to the west coast of Greenland where it becomes the West Greenland Current (Mortensen et al., 2011). The West Greenland current passes ~30 km from the entrance to Godthåbsfjord where it mixes with fjord water causing warm inflow into Godthåbsfjord (Mortensen et al., 2011).

The West Greenland Current water masses are 2–3 °C colder than Irminger Sea water (Rignot et al., 2012), as a result of lateral exchange of heat with the Labrador Sea (Figures 1 and 7; Myers et al., 2007). The West Greenland Current transport of Irminger Sea water into fjords has previously been described from other

Journal of Geophysical Research: Biogeosciences 10.1029/2018JG004385

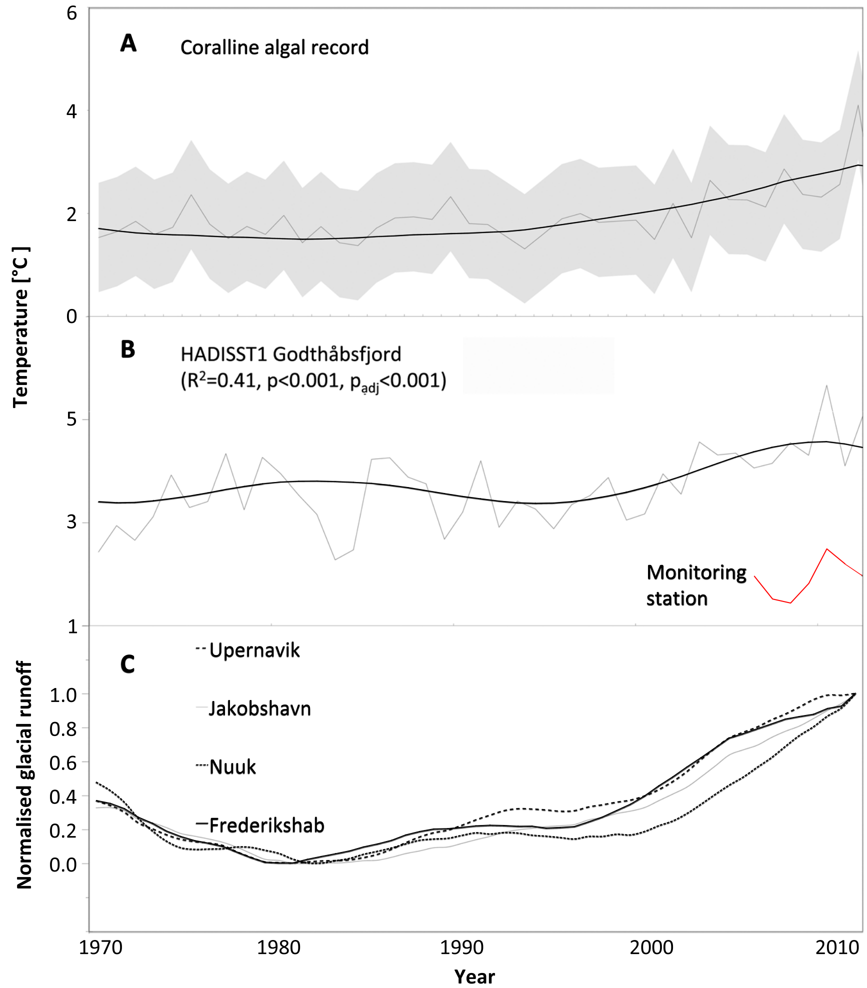

Figure 7. (a) Algal proxy time series (five transects from two samples averaged, May–October). Thick lines show low frequency reconstructions calculated using singular spectrum analysis. The shaded area shows the error of reconstruction (standard error of calibration). (b) HADISST1 data from Godthåbsfjord (May–October) and oceanographic monitoring station (12-m depth) data (May–October). The *r* and *p* values represent correlations of coralline algal time series (samples 5c and 6a averaged) to HADISST1. (c) Low-frequency trends of normalized runoff from four tidewater glaciers based on Noël et al. (2015) model data.

West Greenland fjords (Holland et al., 2008). This intrusion of water masses with temperatures 5 °C higher than surrounding water can influence melting and therefore runoff from tidewater glaciers. From August to mid-October, when *C. compactum* growth rates are the highest, circulation in Godthåbsfjord is a combination of estuarine (deep inflow and shallow outflow driven by a density gradient as a result of subglacial discharge) and intermediate baroclinic circulation (flow driven by tidal mixing causing differing density between the outer sill region of the main fjord and the shelf; Mortensen et al., 2014). When intermediate baroclinic circulation occurs, shelf water passes over the turbulent outer sill region of the fjord extending to the base of the outlet glaciers, contributing to melting, and hence eastward beyond the algal collection site (Mortensen et al., 2014) allowing for the shelf water to influence both algal Mg/Ca and glacial runoff.

Comparisons between coralline algal Mg/Ca and Godthåbsfjord SST reveal local temperature to have a significant influence on Mg/Ca incorporation into the algal calcitic skeleton, with a standard error of the Mg/Ca-temperature calibration of 1.06 °C. While correlations between the coralline algal time series and SST (and runoff) are significant, it is the general trend of the environmental factors that is reflected, rather than year-to-year variability. In addition to temperature, 62% of the variability in Mg/Ca is explained by other factors, such as light. The influence of light on coralline algal growth, and therefore Mg/Ca incorporation, has been demonstrated previously (Adey, 1970; Halfar et al., 2011; Moberly, 1968), and local and temporal shadings by macroalgae, or factors such as cloud cover variability (Burdett et al., 2011), may be influencing specimen specific growth rates.

Fluctuations in SST have a notable effect on meltwater runoff from tidewater glaciers (Drinkwater et al., 2014; Howat et al., 2008; Kerr, 2000). Hence, the coralline algal Mg/Ca ratios track glacial runoff time series via the SST variability, which in turn is linked to air temperatures. A similar temperature-runoff relationship has previously been recorded with a different species of coralline algae in Greenland (Søndre Strømfjord) using a paired Mg/Ca-δ^{18}O time series to develop a salinity record (Kamenos et al., 2012). This was based on the assumption that Mg/Ca ratios reflect a pure temperature signal, whereas δ^{18}O values represent a mixed salinity and temperature signal. By subtracting the Mg/Ca ratios from δ^{18}O values, the residual was interpreted as a salinity signal. The Søndre Strømfjord study found a significant negative correlation between salinity and glacial runoff (Kamenos et al., 2012). Unlike in the present study, algal temperatures recorded in the southwestern Greenland fjord were negatively correlated with atmospheric temperatures. This was interpreted as a result of cold meltwater decreasing temperatures in water layers driven by runoff (Kamenos et al., 2012). Instead, the coralline algal temperatures derived in our study are driven by ocean temperatures which in turn affect glacial runoff via both ocean and air temperatures. This can be confirmed by oceanographic monitoring station data exhibiting a negative correlation between temperature and salinity ($r = -0.63$, $n = 602$, $p < 0.001$), suggesting more runoff occurs at higher water temperatures. A similar temperature-runoff relationship was postulated based on an ice-sheet runoff model for the Nuuk (Kangiata Nunaata Sermia, Akugdlerssûp Sermia, and Narsap Sermia) and Ilulissat (Jakobshavn) glaciers (Hanna et al., 2011, 2013).

5. Conclusions

The time series presented here was limited to the past 42 years, but *C. compactum* is known to have a lifespan of up to 650 years (Halfar et al., 2013). *C. compactum* is abundant along the western and eastern Greenland coasts as far north as Upernavik (Jørgensbye & Halfar, 2016), and samples with lifespans exceeding 100 years have recently been collected in this region (J. Halfar pers. obs.). The coralline algal Mg/Ca proxy enables estimation of local ocean temperatures, which in turn influence glacial runoff of west Greenland tidewater glaciers. The relatively large error associated with coralline algal Mg/Ca records can be reduced by averaging of a larger number of samples, to reduce the impact of specimens specific variability on the quality of the reconstructions. Since changes in temperature of 1.06 °C can be resolved, which is comparable to other marine temperature proxies (e.g., Flannery et al., 2017), this proxy's sensitivity exceeds the magnitude of expected future global warming in the arctic (arctic amplification) and also exceeds the magnitude of changes that have taken place since the beginning of the anthropogenic impact on the climate system. Additionally, a lack of runoff records prior to 1950 makes *C. compactum* a promising high-resolution proxy that can help place the currently ongoing precipitous decline of Greenland ice mass (Morlighem et al., 2017) into a long-term context. Hence, with the collection of samples with longer uninterrupted lifespans, *C. compactum* is a promising climate archive for improving our understanding of past changes in Greenland ocean and ice sheet conditions well before the beginning of instrumental observations.

Acknowledgments
The authors declare no competing interests. Coralline algal Mg/Ca and model output runoff data are available in supporting information. We acknowledge the marine monitoring program MarineBasis-Nuuk, part of the Greenland Ecosystem Monitoring, for supplying the in situ temperature data. This work was funded by the Centre for Global Change Science; the Geological Society of America; and a Natural Sciences and Engineering Research Council of Canada Discovery grant to J. H.

References

Adey, W. H. (1970). The effects of light and temperature on growth rates in boreal-subarctic crustose corallines. *Journal of Phycology*, *9*, 269–276.

Adey, W. H., Halfar, J., & Williams, B. (2013). The coralline genus *Clathromorphum* foslie emend. Adey, Smithson. *Contributions in Marine Science*, *40*, 1–41.

Buch, E., Pedersen, S. A., & Ribergaard, M. H. (2004). Ecosystem variability in West Greenland waters. *Journal of Northwest Atlantic Fishery Science*, *34*, 13–28. https://doi.org/10.2960/J.v34.m479

Burdett, H., Kamenos, N. A., & Law, A. (2011). Using coralline algae to understand historic marine cloud cover. *Palaeogeography Palaeoclimatology Palaeoecology*, *302*(1–2), 65–70. https://doi.org/10.1016/j.palaeo.2010.07.027

Cuny, J., Rhines, P. B., Niiler, P. P., & Bacon, S. (2002). Labrador Sea boundary currents and the fate of the Irminger Sea water. *Journal of Physical Oceanography*, *32*(2), 627–647. https://doi.org/10.1175/1520-0485(2002)032%3C0627:lsbcat%3E2.0.co;2

Drinkwater, K. F., Miles, M., Medhaug, I., Otterå, O. H., Kristiansen, T., Sundby, S., & Gao, Y. (2014). The Atlantic multidecadal oscillation: Its manifestations and impacts with special emphasis on the Atlantic region north of 60°N. *Journal of Marine Systems*, *133*, 117–130. https://doi.org/10.1016/j.jmarsys.2013.11.001

ECMWF-IFS: ECMWF-IFS (2008): Part IV: Physical processes (CY33R1), Technical Report.

Enderlin, E. M., Howat, I. M., Jeong, S., Noh, M.-J., van Angelen, J. H., & Van den Broeke, M. R. (2014). An improved mass budget for the Greenland ice sheet. *Geophysical Research Letters*, *41*, 866–872. https://doi.org/10.1002/2013GL059010

Enderlin, E. M., Howat, I. M., & Vieli, A. (2013). High sensitivity of tidewater outlet glacier dynamics to shape. *The Cryosphere*, *7*(3), 1007–1015. https://doi.org/10.5194/tc-7-1007-2013

Flannery, J. A., Richey, J. N., Thirumalai, K., Poore, R. Z., & DeLong, K. L. (2017). Multi-species coral Sr/Ca-based sea-surface temperature reconstruction using *Orbicella faveolata* and *Siderastrea siderea* from the Florida Straits. *Palaeogeography Palaeoclimatology Palaeoecology*, *466*, 100–109. https://doi.org/10.1016/j.palaeo.2016.10.022

Gamboa, G., Halfar, J., Hetzinger, S., Adey, W. H., Zack, T., Kunz, B. E., & Jacob, D. E. (2010). Mg/Ca ratios in coralline algae record northwest Atlantic temperature variations and North Atlantic Oscillation relationships. *Journal of Geophysical Research*, *115*, C12044. https://doi.org/10.1029/2010JC006262

Halfar, J., Adey, W. H., Kronz, A., Hetzinger, S., Edinger, E., & Fitzhugh, W. W. (2013). Arctic sea-ice decline archived by multicentury annual-resolution record from crustose coralline algal proxy. *Proceedings of the National Academy of Sciences*, *110*(49), 19,737–19,741. https://doi.org/10.1073/pnas.1313775110

Halfar, J., Steneck, R. S., Joachimski, M., Kronz, A., & Wanamaker, A. D. (2008). Coralline red algae as high-resolution climate recorders. *Geology*, *36*(6), 463–466. https://doi.org/10.1130/G24635A.1

Halfar, J., Williams, B., Hetzinger, S., Steneck, R. S., Lebednik, P. A., Winsborough, C., et al. (2011). 225 years of Bering Sea climate and ecosystem dynamics revealed by coralline algal growth-increment widths. *Geology*, *39*(6), 579–582. https://doi.org/10.1130/G31996.1

Hanna, E., Huybrechts, P., Cappelen, J., Steffen, K., Bales, R. C., Burgess, E. W., et al. (2011). Greenland ice sheet surface mass balance 1870 to 2010 based on twentieth century reanalysis, and links with global climate forcing. *Journal of Geophysical Research*, *116*, D24121. https://doi.org/10.1029/2011JD016387

Hanna, E., Huybrechts, P., Steffen, K., Cappelen, J., Huff, R., Shuman, C., et al. (2008). Increased runoff from melt from the Greenland ice sheet: A response to global warming. *Journal of Climate*, *21*(2), 331–341. https://doi.org/10.1175/2007JCLI1964.1

Hanna, E., Jones, J. M., Cappelen, J., Mernild, S. H., Wood, L., Steffen, K., & Huybrechts, P. (2013). The influence of North Atlantic atmospheric and oceanic forcing effects on 1900–2010 Greenland summer climate and ice melt/runoff. *International Journal of Climatology*, *33*(4), 862–880. https://doi.org/10.1002/joc.3475

Hetzinger, S., Halfar, J., Kronz, A., Simon, K., Adey, W. H., & Steneck, R. S. (2018). Reproducibility of *Clathromorphum compactum* coralline algal Mg/Ca ratios and comparison to high-resolution sea surface temperature data. *Geochimica et Cosmochimica Acta*, *220*, 96–109. https://doi.org/10.1016/j.gca.2017.09.044

Hetzinger, S., Halfar, J., Kronz, A., Steneck, R. S., Adey, W. H., Lebednik, P. A., & Schöne, B. R. (2009). High-resolution Mg/Ca ratios in a coralline red alga as a proxy for Bering Sea temperature variations from 1902 to 1967. *Palaios*, *24*(6), 406–412. https://doi.org/10.2110/palo.2008.p08-116r

Holland, D. M., Thomas, R. H., de Young, B., Ribergaard, M. H., & Lyberth, B. (2008). Acceleration of Jakobshavn Isbræ triggered by warm subsurface ocean waters. *Nature Geoscience*, *1*(10), 659–664. https://doi.org/10.1038/ngeo316

Howat, I. M., Joughin, I., Fahnestock, M., Smith, B. E., & Scambos, T. A. (2008). Synchronous retreat and acceleration of southeast Greenland outlet glaciers 2000–06: Ice dynamics and coupling to climate. *Journal of Glaciology*, *54*(187), 646–660. https://doi.org/10.3189/002214308786570908

Jones, P. D., & Moberg, A. (2003). Hemispheric and large-scale surface air temperature variations: An extensive revision and an update to 2001. *Journal of Climate*, *16*(2), 206–223. https://doi.org/10.1175/1520-0442(2003)016<0206:HALSSA>2.0.CO;2

Jørgensbye, H. I. Ø., & Halfar, J. (2016). Overview of coralline red algal crusts and rhodolith beds (Corallinales, Rhodophyta) and their possible ecological importance in Greenland. *Polar Biology*, 1–15. https://doi.org/10.1007/s00300-016-1975-1

Kamenos, N. A., Hoey, T. B., Nienow, P., Fallick, A. E., & Claverie, T. (2012). Reconstructing Greenland ice sheet runoff using coralline algae. *Geology*, *40*(12), 1095–1098. https://doi.org/10.1130/G33405.1

Kerr, R. A. (2000). A North Atlantic climate pacemaker for the centuries. *Science*, *288*(5473), 1984–1985. https://doi.org/10.1126/science.288.5473.1984

Moberly, R. J. (1968). Composition of magnesian calcites of algae and pelecypods by electron microprobe analysis. *Sedimentology*, *11*(1–2), 61–82. https://doi.org/10.1111/j.1365-3091.1968.tb00841.x

Moore, R. D., & Demuth, M. N. (2001). Mass balance and streamflow variability at Place Glacier, Canada, in relation to recent climate fluctuations. *Hydrological Processes*, *15*(18), 3473–3486. https://doi.org/10.1002/hyp.1030

Morlighem, M., Williams, C. N., Rignot, E., An, L., Arndt, J. E., Bamber, J. L., et al. (2017). Special section: BedMachine v3: Complete bed topography and ocean bathymetry mapping of Greenland from multibeam. *Geophysical Research Letters*, *44*, 1–11. https://doi.org/10.1002/2017GL074954

Mortensen, J., Bendtsen, J., Lennert, K., & Rysgaard, S. (2014). Seasonal variability of the circulation system in a west Greenland tidewater outlet fjord. *Godthabsfjord*, 2591–2603. https://doi.org/10.1002/2014JF003267.Received

Mortensen, J., Bendtsen, J., Motyka, R. J., Lennert, K., Truffer, M., Fahnestock, M., & Rysgaard, S. (2013). On the seasonal freshwater stratification in the proximity of fast-flowing tidewater outlet glaciers in a sub-Arctic sill fjord. *Journal of Geophysical Research: Oceans*, *118*, 1382–1395. https://doi.org/10.1002/jgrc.20134

Mortensen, J., Lennert, K., Bendtsen, J., & Rysgaard, S. (2011). Heat sources for glacial melt in a sub-Arctic fjord (Godthåbsfjord) in contact with the Greenland ice sheet. *Journal of Geophysical Research*, *116*, C01013. https://doi.org/10.1029/2010JC006528

Myers, P. G., Kulan, N., & Ribergaard, M. H. (2007). Irminger water variability in the West Greenland current. *Geophysical Research Letters*, *34*, L17601. https://doi.org/10.1029/2007GL030419

Noël, B., Van De Berg, W. J., Van Meijgaard, E., Kuipers Munneke, P., Van De Wal, R. S. W., & Van Den Broeke, M. R. (2015). Evaluation of the updated regional climate model RACMO2.3: Summer snowfall impact on the Greenland Ice Sheet. *The Cryosphere*, *9*(5), 1831–1844.

Noël, B., van de Berg, W. J., van Wessem, J. M., van Meijgaard, E., van As, D., Lenaerts, J. T. M., et al. (2018). Modelling the climate and surface mass balance of polar ice sheets using RACMO2 – Part 1: Greenland (1958–2016). *The Cryosphere*, *12*, 811–831. https://doi.org/10.5194/tc-12-811-2018

Paillard, D., Labyrie, L., & Yiou, P. (1996). Macintosh program performs time-series analysis. *Eos, Transactions American Geophysical Union*, *77*, 379.

Peterson, T. C. and Vose, R. S., An overview of the Global Historical Climatology Network temperature database, *Bulletin of the American Meteorological Society*, *78*(12), 2837–2849. Retrieved from https://www.ncdc.noaa.gov/ghcnm/v2.php (Accessed 2 May 2016), 1997.

Rayner, N. A., Parker, D. E., Horton, E. B., Folland, C. K., Alexander, L. V., Rowell, D. P., et al. (2003). Global analyses of sea surface temperature, sea ice, and night marine air temperature since the late nineteenth century. *Journal of Geophysical Research*, *108*(D14), 4407. https://doi.org/10.1029/2002JD002670

Reynolds, R. W., Rayner, N. A., Smith, T. M., Stokes, D. C., & Wang, W. (2002). An improved in situ and satellite SST analysis for climate. *Journal of Climate*, *15*(13), 1609–1625. https://doi.org/10.1175/1520-0442(2002)015<1609:AIISAS>2.0.CO;2

Rignot, E., Fenty, I., Menemenlis, D., & Xu, Y. (2012). Spreading of warm ocean waters around Greenland as a possible cause for glacier acceleration. *Annals of Glaciology*, *53*(60), 257–266. https://doi.org/10.3189/2012AoG60A136

Vautard, R., Yiou, P., & Ghil, M. (1992). Singular-spectrum analysis: A toolkit for short, noisy chaotic signals. *Physica D*, *58*(1–4), 95–126. https://doi.org/10.1016/0167-2789(92)90103-T

Williams, B., Halfar, J., DeLong, K. L., Hetzinger, S., Steneck, R. S., & Jacob, D. E. (2014). Multi-specimen and multi-site calibration of Aleutian coralline algal Mg/Ca to sea surface temperature. *Geochimica et Cosmochimica Acta*, *139*, 190–204. https://doi.org/10.1016/j.gca.2014.04.006

Williams, S., Halfar, J., Zack, T., Hetzinger, S., Blicher, M., & Juul-Pedersen, T. (2018). Comparison of climate signals obtained from encrusting and free-living rhodolith coralline algae. *Chemical Geology*, *476*, 418–428. https://doi.org/10.1016/j.chemgeo.2017.11.038

Xu, Y., Rignot, E., Menemenlis, D., & Koppes, M. (2012). Numerical experiments on subaqueous melting of Greenland tidewater glaciers in response to ocean warming and enhanced subglacial discharge. *Annals of Glaciology*, *53*(60), 229–234. https://doi.org/10.3189/2012AoG60A139